

General Methodology to Optimize Damping Functions to Account for Charge Penetration Effects in Electrostatic Calculations Using Multicentered Multipolar Expansions

Araken S. Werneck,[†] Tarcísio M. Rocha Filho,[‡] and Laurent E. Dardenne^{*,§}

Departamento de Física, Universidade Católica de Brasília, UCB, Brazil, Instituto de Física, Universidade de Brasília, UnB, Brazil, and Laboratório Nacional de Computação Científica—LNCC/MCT, Av Getúlio Vargas 333 Quitandinha Petrópolis, RJ CEP: 25651-071, Brazil

Received: July 16, 2007; In Final Form: September 4, 2007

We developed a methodology to optimize exponential damping functions to account for charge penetration effects when computing molecular electrostatic properties using the multicentered multipolar expansion method (MME). This methodology is based in the optimization of a damping parameter set using a two-step fast local fitting procedure and the *ab initio* (Hartree–Fock/6-31G** and 6-31G**+) electrostatic potential calculated in a set of concentric grid of points as reference. The principal aspect of the methodology is a first local fitting step which generates a focused initial guess to improve the performance of a simplex method avoiding the use of multiple runs and the choice of initial guesses. Three different strategies for the determination of optimized damping parameters were tested in the following studies: (1) investigation of the error in the calculation of the electrostatic interaction energy for five hydrogen-bonded dimers at standard and nonstandard hydrogen-bonded geometries and at nonequilibrium geometries; (2) calculation of the electrostatic molecular properties (potential and electric field) for eight small molecular systems (methanol, ammonia, water, formamide, dichloromethane, acetone, dimethyl sulfoxide, and acetonitrile) and for the 20 amino acids. Our results show that the methodology performs well not only for small molecules but also for relatively larger molecular systems. The analysis of the distinct parameter sets associated with different optimization strategies show that (i) a specific parameter set is more suitable and more general for electrostatic interaction energy calculations, with an average absolute error of 0.46 kcal/mol at hydrogen-bond geometries; (ii) a second parameter set is more suitable for electrostatic potential and electric field calculations at and outside the van der Waals (vdW) envelope, with an average error decrease >72% at the vdW surface. A more general amino acid damping parameter set was constructed from the original damping parameters derived for the small fragments and for the amino acids. This damping set is more insensitive to protein backbone and residue side-chain conformational changes and can be very useful for future docking and molecular dynamics protein simulations using *ab initio* based polarizable classical methods.

Introduction

Electrostatic effects are of central importance in determining the structure and function of biomolecules and play a major role in a variety of functional mechanisms associated with proteins^{1–3} (e.g., molecular recognition, ligand specificity, enzyme catalytic mechanism, and regulation). A correct treatment of electrostatic interactions is a central point in the development of biomolecular force fields, but their accuracy is often limited by the use of the atom-centered charge approximation, i.e., charges placed only at the atomic centers and obtained either from *ab initio* quantum mechanical calculations or by empirical parametrization. A more precise way to compute molecular electrostatic properties makes use of multicentered multipolar expansions (MME) to represent the charge distribution associated with a precomputed *ab initio* quantum wave function.^{4–15} It is also computationally faster than the exact *ab initio* procedure and can exhibit a high degree of accuracy depending on the level of the multipolar expansion (i.e.,

monopole, dipole, quadrupole, octupole, ..., terms) and the number of expansion points taken (usually atom and bond midpoints are taken as expansion centers). The multicenter multipolar electrostatic model is employed in pseudoquantum potentials and also in hybrid QM/MM (quantum mechanic/molecular mechanic) methodologies as in the effective fragment potential (EFP) method.^{10–14,16}

The calculation of electrostatic properties using the MME approach has two critical aspects when we are interested to study biological macromolecules and even molecules of moderate size. The first one is the necessity to treat the whole macromolecule by a reassociation of fragments method in order to avoid a whole molecule *ab initio* calculation (frequently beyond the available computational resources). This point was focused by two of us in the development of the OME (overlapping of multipolar expansions) reassociation method,¹⁷ which was used in the investigation of the papain catalytic mechanism.²⁰ Moreover, divide-and-conquer approaches were also developed by other groups to treat biological macromolecules.^{16,19} A second critical aspect is the necessity to account for charge penetration effects in order to calculate accurate electrostatic properties at short distances from molecular expansion centers. In fact, at short distances (e.g., van der Waals distances and hydrogen-bonding

* Corresponding author. E-mail: dardenne@lncc.br. Phone: (55) 24 22336009. Fax: (55) 24 22336165.

[†] Universidade Católica de Brasília.

[‡] Universidade de Brasília.

[§] Laboratório Nacional de Computação Científica.

distances) the accuracy of electrostatic properties calculated using the MME method decreases considerably and errors due to charge penetration effects become more relevant. Charge penetration correction is necessary for the application of the MME method in several important studies where we need a correct evaluation of electrostatic interaction energies, electrostatic potentials, and electric fields at relatively short-range distances. Some important applications include the accurate computation of the electrostatic interaction energy in simulating systems with intra- and intermolecular hydrogen-bond formation, as in chemical reactions, clusters of solvent molecules, solvated biomolecular systems, and ligand–receptor docking studies; the computation of electrostatic potentials and electric fields at molecular van der Waals (vdW) distances in active-site electrostatic studies; investigation of electrostatic properties of ligand molecular vdW surfaces and inclusion of solvent effects using continuum boundary element methods.²⁰ Moreover, electrostatic potential/electric field damping strategies are also an important aspect for the development of polarizable molecular mechanics force fields.^{10,21–33,41}

A possible way to account for charge penetration effects, using the MME method, is to introduce distance dependent damping functions associated with each multipolar expansion center.^{10,21,22} Freitag et al.²¹ proposed a damping function, $f^{\text{damp}} = 1.0 - \exp(-\alpha_i r)$, and derived the formula to calculate the electrostatic interaction energy between two fragment molecules. The authors tested their method with success for five dimers of small solvent molecules and also proposed a protocol to obtain optimal exponential α_i damping parameters. In the present paper we developed, based on the work of Freitag et al., a straightforward and numerically efficient methodology to optimize exponential damping functions of the form f^{damp} , to account for charge penetration effects. The methodology is general and can be applied not only to small solvent molecules but also to molecules of moderate size. The number of expansion points, associated with the MME method, increases with the size of the molecule, and the methodology used to obtain an optimal set $\{\alpha_i\}$ of damping parameters becomes crucial. We investigate three different strategies for the determination of the set $\{\alpha_i\}$ of optimized damping parameters and investigate their success, relative to the ab initio values, to correct the MME method in evaluating the electrostatic potential and the electric field (intensity and direction) in regions inside, outside, and inside/outside the vdW envelope. We tested our methodology in eight small solvent molecules (water, ammonia, methanol, dichloromethane, acetone, dimethyl sulfoxide, acetonitrile, and formamide) and also in the set of 20 amino acids. The error in the calculation of the electrostatic interaction energy, using the Morokuma analysis³⁴ as reference, was analyzed for five dimers (water–water; water–ammonia, water–formamide, methanol–methanol, and formamide–formamide) at their standard hydrogen-bonded geometries and also for water–water and formamide–formamide dimers at nonequilibrium geometries.

Computational Methodology

In the present paper the multicentered multipolar (up to octupoles) expansions (MME) are derived from ab initio Hartree–Fock/6-31G** and /6-31G**+ wave functions considering the atomic positions and the middle of each chemical bond as expansion centers. The standard expression, for each expansion point, used for the evaluation of the electrostatic potential (eq 1) is multiplied by the damping function $f^{\text{damp}} = [1 - \exp(-\alpha_i r_{iA})]$ to correct the MME electrostatic model (eq 2) to account for charge penetration errors at short distances.

$$V^{\text{mult}}(\mathbf{r}_A) = \sum_{i=1}^N [V_i^0(r_{iA}) + V_i^1(r_{iA}) + V_i^2(r_{iA}) + V_i^3(r_{iA})] \quad (1)$$

$$V^{\text{damp-mult}}(\mathbf{r}) = \sum_{i=1}^N (1 - e^{-\alpha_i r_{iA}}) \left[\sum_{j=1}^3 V_i^j(r_{iA}) \right] \quad (2)$$

where N is the number of expansion points in the fragment/molecule, the superscripts 0, 1, 2, and 3 stand for the monopolar, dipolar, quadrupolar, and octupolar contributions, respectively, and r_{iA} is the distance of the evaluation point \mathbf{r} from the expansion point i .

The total electrostatic interaction energy E^{inter} between two fragments can be evaluated using the following expressions derived by Freitag et al.:

$$E^{\text{mult}} \cong \sum_{i=1}^{N_1} \sum_{j=1}^{N_2} \left\{ \frac{q_i q_j}{r_{ij}} \left[1 - \frac{(e^{-\alpha_i r_{ij}} + e^{-\alpha_j r_{ij}})}{2} - \frac{(\alpha_i^2 + \alpha_j^2)}{2(\alpha_i^2 - \alpha_j^2)} (e^{-\alpha_j r_{ij}} - e^{-\alpha_i r_{ij}}) \right] + \frac{q_i Z_j}{r_{ij}} [1 - e^{-\alpha_j r_{ij}}] + \frac{q_j Z_i}{r_{ij}} [1 - e^{-\alpha_i r_{ij}}] \right\} + \sum_{i=1}^{N_1} \sum_{j=1}^{N_2} \left\{ \frac{Z_i Z_j}{r_{ij}} + \sum_{n=1}^3 E_{0,i}^{n,j} + \sum_{n=1}^3 E_{n,i}^{0,j} + \sum_{n=1}^3 E_{1,i}^{n,j} + \sum_{n=1}^3 E_{n,i}^{1,j} + E_{2,i}^{2,j} \right\} \quad (3)$$

for $\alpha_i \neq \alpha_j$, where N_1 and N_2 are the number of expansion centers for fragment 1 and 2, respectively; r_{ij} is the distance between expansions centers i and j ; q_i (q_j) is the charge associated to the monopolar contribution from expansion center i (j) and fragment 1 (fragment 2) and Z is the nuclear charge ($Z = 0$ for bond midpoints expansion centers). The $E_{n,i}^{m,j}$ terms are the electrostatic interactions between the n -multipolar moment (from expansion center i —fragment 1) and the m -multipolar moment (center j —fragment 2).

$$E^{\text{inter}} \cong \sum_{i=1}^{N_1} \sum_{j=1}^{N_2} \left\{ \frac{q_i q_j}{r_{ij}} \left[1 - e^{-\alpha r_{ij}} \left(1 + \frac{\alpha r_{ij}}{2} \right) \right] + \frac{(q_i Z_j + q_j Z_i)}{r_{ij}} [1 - e^{-\alpha r_{ij}}] \right\} + \sum_{i=1}^{N_1} \sum_{j=1}^{N_2} \left\{ \frac{Z_i Z_j}{r_{ij}} + \sum_{n=1}^3 E_{0,i}^{n,j} + \sum_{n=1}^3 E_{n,i}^{0,j} + \sum_{n=1}^3 E_{1,i}^{n,j} + \sum_{n=1}^3 E_{n,i}^{1,j} + E_{2,i}^{2,j} \right\} \quad (4)$$

for $\alpha_i = \alpha_j = \alpha$.

Expressions 3 and 4 for the electrostatic interaction energies incorporate only charge–charge and nuclear–charge corrections for charge penetration effects. In our analyses higher order terms for the electrostatic interaction energy are used without correction. In their paper Freitag et al. argued that even with this severe truncation a major percentage of the total charge penetration error is still corrected.

Optimization Procedure of Damping Parameters. The objective is to obtain, for a particular molecular system, an optimal set of damping parameters $\{\alpha_i\}$ minimizing the difference between the ab initio V^{ab} potential and the damped MME electrostatic potential calculated in a set of grid of points

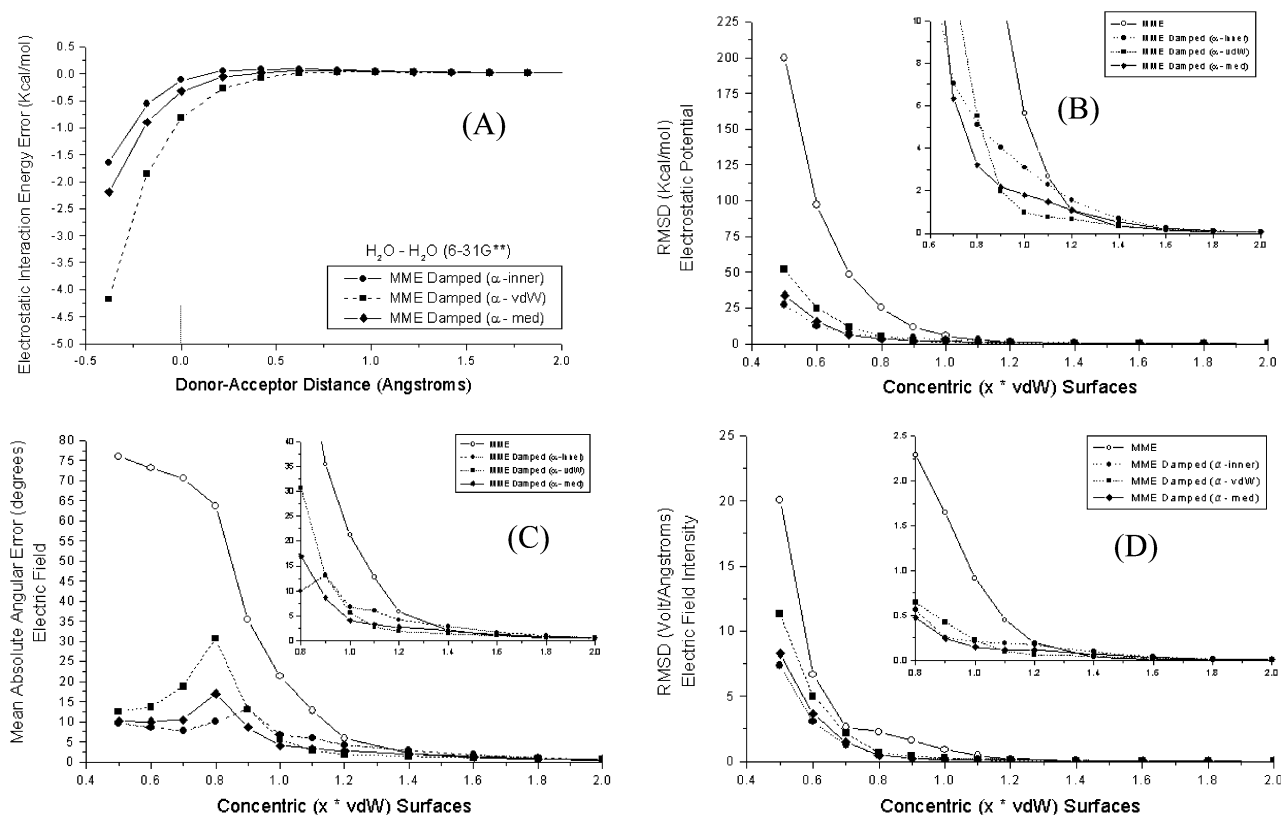


Figure 1. Electrostatic interaction energy, potential, and electric field water dimer study. (A) The electrostatic interaction energy error (kcal/mol), where the energies of MME are compared to the Morokuma procedure. (B) The rmsd for the electrostatic potential (kcal/mol) where the MME procedures is compared to the ab initio procedure. The decrease in the error is analyzed at the concentric surfaces. (C) The mean absolute angular error (degrees) of the electric field where the MME procedure is compared to the ab initio procedure also analyzed at the concentric surfaces. (D) The rmsd of the electric field intensity is also compared to the ab initio procedure and also analyzed at the concentric surfaces. In the panels B–D we present a more detailed analysis for the concentric surfaces ranging from 0.8 to 2.0 Å. The symbol $x \cdot \text{vdW}$ represents the scaled van der Waals radii. Results obtained using the 6-31G** basis set.

(defined about a particular fragment molecule). The error function is defined by

$$\Delta = \sum_{k=1}^{N_p} [V^{\text{ab}}(r_k) - V^{\text{damp-mult}}(r_k, \{\alpha_i\})]^2; \quad N_p = \text{number of grid points} \quad (5)$$

The minimization of the error Δ as a function of the parameter set $\{\alpha_i\}$ is a very hard optimization problem to solve even for a moderate size molecule with several multipolar expansions centers. It is not obvious that a particular global optimization methodology is feasible in this case with a reasonable computational cost.

Here we present a general two-step local fitting procedure to optimize the set $\{\alpha_i\}$ of parameters. Basically the methodology consists of the following two steps:

(I) A first set $\{\alpha_i^1\}$ is generated using a fast iterative procedure where each α_i parameter is optimized using only the ab initio and MME calculated values at grid points with a distance ≤ 1.8 Å from the respective expansion point.

(II) The $\{\alpha_i^1\}$ set is used as starting point for a local minimization procedure using an adapted simplex algorithm to obtain a final set of optimized parameters.

Each step is detailed below.

Grid Points Definition. For a particular molecule, 12 concentric grid of points were generated using the Connolly algorithm³⁵ (1.4 Å for the probe radius and a density of 5 points per Å²) and using the vdW atomic radius scaled by a factor $f = 0.5, 0.6, 0.7, 0.8, 0.9, 1.0, 1.1, 1.2, 1.4, 1.6, 1.8,$ and 2.0 for

each concentric surface. The use of small f factors ranging from 0.5 to 0.7 is necessary to obtain results closer to ab initio ones in electrostatic interaction energy calculations for dimers at their standard hydrogen-bonded geometries. In this work we used the following values for the vdW atomic radius: H = 1.2 Å, C = 1.5 Å, N = 1.5 Å, O = 1.4 Å, and S = 1.75 Å. Only the six inner surfaces are considered in the $\{\alpha_i\}$ optimization procedure; the others are used to evaluate the methodology.

First Step Local Fitting. The first step local fitting is an iterative procedure, which can be summarized as follows:

(0) Generation of grid points.

(1) Selection, for each particular expansion center i ($i = 1, \dots, N$), of all grid points k with a distance $r_{ik} \leq 1.8$ Å from center i and with $r_{jk} > r_{ik}$ for all $j \neq i$.

(2) At each grid point selected we calculate V^{ab} and V^{mult} (total multipolar contribution from each molecular expansion center).

(3) For all grid points k selected for a particular expansion center i (on average ~ 100 grid points) we calculated the damping parameter α_i^k using the following expression:

$$\alpha_i^k = -\frac{1}{r_{ik}} \ln \left[1 - \frac{V^{\text{ab}}(\mathbf{r}_{ik}) - \sum_{m \neq i}^N [(1 - e^{-\alpha_m r_{mk}}) \sum_{j=0}^3 V_m^j(r_{mk})]}{\sum_{j=0}^3 V_i^j(r_{ik})} \right] \quad (6)$$

where $V^{\text{ab}}(\mathbf{r}_{ik})$ is the ab initio value precomputed at point \mathbf{r}_{ik} ; r_{mk} is the distance from center m to point k . The derivation of

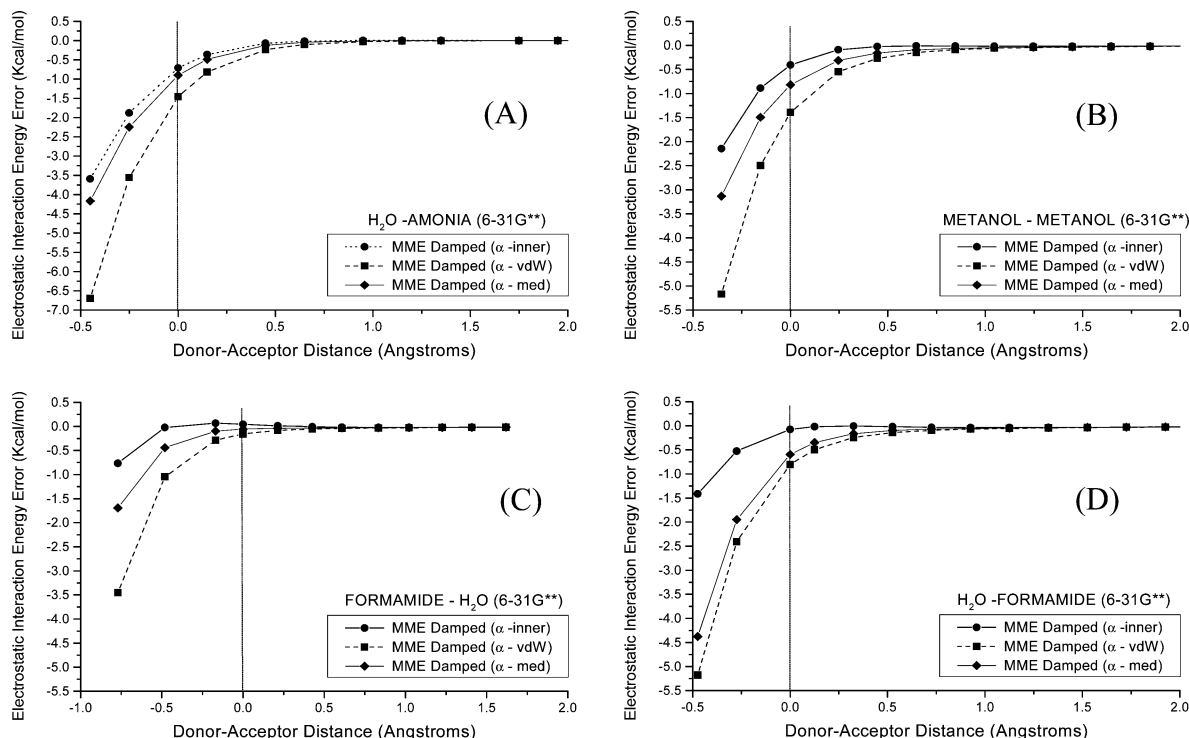


Figure 2. Electrostatic interaction energy error analysis for the dimer molecules: panels A–D present the electrostatic interactions energy error, where the MME energies are compared to the Morokuma procedure. (A) Ammonia–water dimer, (B) methanol dimer, (C) formamide–water dimer, where the water molecule is the acceptor, and (D) formamide–water dimer where the water molecule is the donor. Results obtained using the 6-31G** basis set.

eq 6 follows straightforward from eq 2, assuming that $V^{\text{ab}}(\mathbf{r}_{ik}) - V^{\text{damp-mult}}(\mathbf{r}_{ik}) = 0$. If the logarithm argument in eq 6 becomes negative, the corresponding α_i^k value is not updated.

The starting $\{\alpha_i^k\}$ values for the iterative procedure are obtained using

$$\alpha_i^k = -\frac{1}{r_{ik}} \ln \left[1 - \frac{V^{\text{ab}}(\mathbf{r}_{ik}) - \sum_{m \neq i}^N \sum_{j=0}^3 V_m^j(r_{mk})}{\sum_{j=0}^3 V_i^j(r_{ik})} \right] \quad (7)$$

This equation is similar to eq 6 but the multipolar contributions from the $m \neq i$ centers are considered nondamped. In the first iterative cycle, if the argument of the logarithm in eq 7 is negative or greater than one for some α_i^k , the corresponding grid point is discarded.

(4) Calculation of the mean value for each α_i^k :

$$\alpha_i = \frac{\sum_{k=1}^{M_i} \alpha_i^k}{M_i} \quad (8)$$

where M_i is the number of grid points associated to center i . In our implementation we took account of chemically equivalent multipolar centers (symmetries) in such a way that the corresponding α_i parameters are always equal. For example: if two centers i and j are chemically equivalent we consider a same α parameter for these two centers, and in eq 8 for the derivation of this parameter we consider all the grid points associated to center i and center j with $M = M_i + M_j$. For expansion centers i with $M_i = 0$ and no equivalent centers we fix a value of $\alpha_i = 10$.

(5) Stop the procedure if all α_i satisfy a convergence criterion (in this work, an absolute difference $< 10^{-3}$ for each α_i). Otherwise return to step 3.

It is important to note that in the first optimization step described above the α_i^k damping parameters associated to the i th multipolar center are derived using the electrostatic potential calculated only at grid points close $r_{ik} \leq 1.8 \text{ \AA}$ to the respective expansion point. The first local fitting step assumes that at short distances to a particular expansion center the MME damping error is almost completely due to this particular multipolar expansion. This is only an approximation because in molecular systems we have situations where the penetration error is due to two or more multipolar expansion points which are very close to each other.

Second Step Local Minimization. The set $\{\alpha_i^1\}$ is used as an initial guess for a local minimization procedure using an adapted downhill simplex algorithm³⁶ to obtain a final set of optimized parameters. We chose to use the downhill simplex method. A simplex is the geometrical figure formed by the connecting segments of $N + 1$ vertices in N dimensions. We start with the simplex formed by the initial guess and the points obtained from it by displacements of length L in the directions of each coordinate axis. The method then consists in changing the vertices according to the following predefined rules to obtain the (local) minimum of a function, in our case the error function Δ as given in eq 5:

- (i) Compute the values of Δ at each vertex. Locate the vertex with worst (maximal) value of the function Δ .
- (ii) Move this point by a reflection through the opposite face.
- (iii) If the new point is lower than the best value then try a reflection by a factor 2.
- (iv) If the reflected point is worse than the second highest point, then contract the vertex by a factor of one-half with respect to the opposite face.

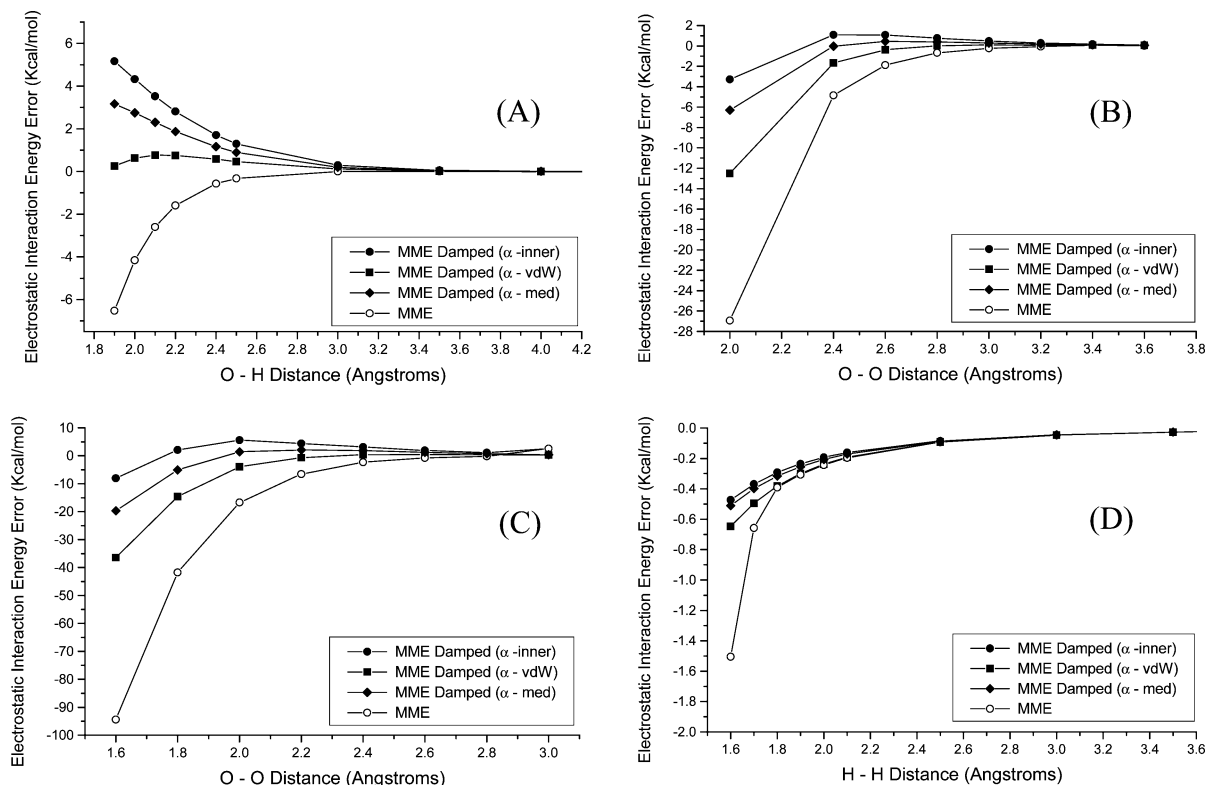


Figure 3. Electrostatic interaction energy error analysis for four water dimer configurations. The MME energies are compared to the Morokuma procedure. Water dimer configurations for A, B, C, and D are represented in panels A, B, C, and D, respectively. Results obtained using the 6-31G** basis set.

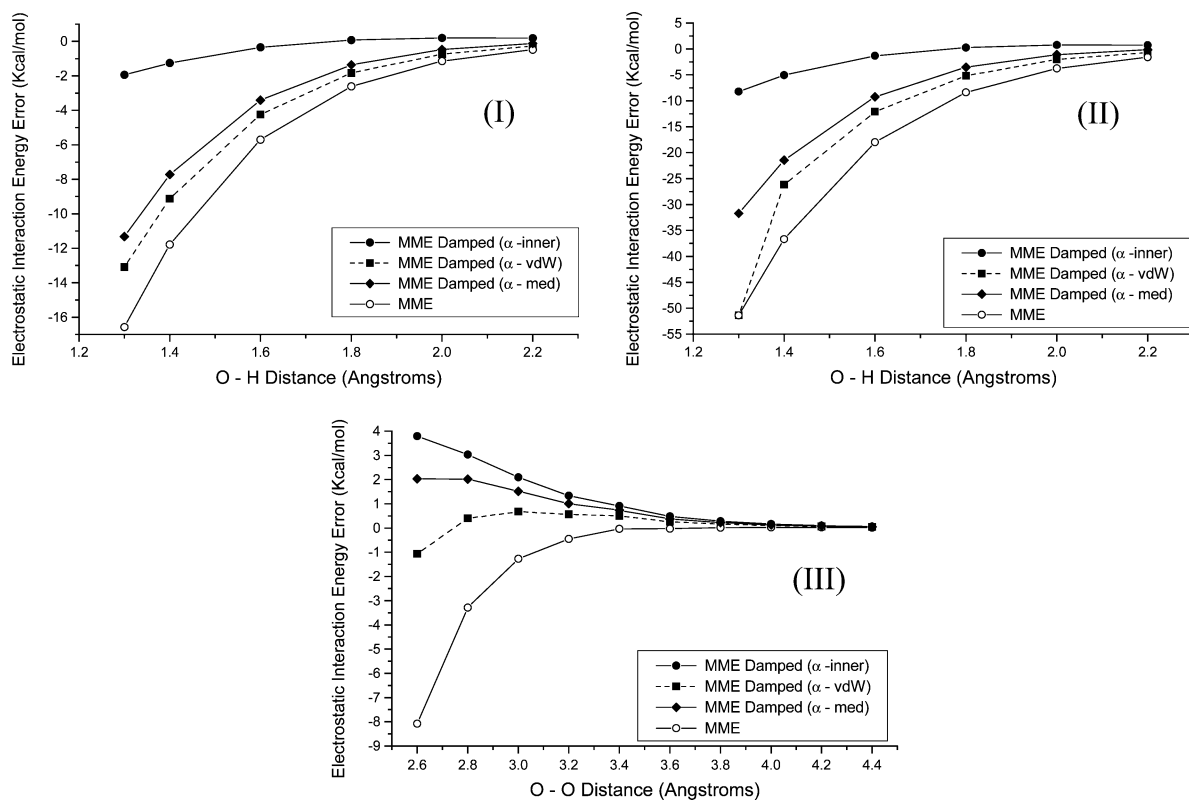


Figure 4. Electrostatic interaction energy error analysis for three formamide dimer configurations. The MME energies are compared to the Morokuma procedure. Formamide dimers configurations for I, II, and III are represented in panels I, II, and III, respectively. The H-bonded geometry (I) presents a minima at the 2.0 O-H distance. Results obtained using the 6-31G** basis set.

(v) If this new point is still the worse, then contract the whole simplex by a factor around the best point. Return to step i.

These steps are repeated until the minimal value of Δ obtained stops varying up to some tolerance or if we reach the predefined

maximal number of iterations of the algorithm. In our approach we also consider the chemically equivalent multipolar centers (i.e., centers which have the same value for the α_i parameters). The value of L in the initial simplex is determined by the scale

length of the problem. In our case we chose $L = 0.1$ which is typically 1 order of magnitude smaller than the parameters α_i obtained as first guess. The maximal number of iterations can vary according to the desired accuracy and is of the order of 7000. The tolerance for the relative variation of the error function Δ is 10^{-6} and all the grid points are used in the computation of the error function Δ . The CPU time for the whole procedure ranges from a few seconds for small molecules (water, ammonia, formamide, methanol) to a few minutes for the amino acid systems, in a 1.2 GHz Pentium 4 computer. It is important to note that the simplex method explores a finite region of the parameter space around the best point obtained yet, but can in many cases escape to a lower local minimum, although not a global minimum.

Damping Parameter Sets. We tested and analyzed three distinct ways to obtain optimized damping parameters sets using the optimization procedure described above:

(i) $\{\alpha_i\}^{\text{inner}}$ parameter set: obtained using the five inner concentric molecular surfaces of grid points (constructed with the atomic vdW radii scaled by a factor ranging from 0.5 to 0.9).

(ii) $\{\alpha_i\}^{\text{vdW}}$ parameter set: obtained using only points at the vdW molecular surface.

(iii) $\{\alpha_i\}^{\text{med}}$ parameter set: obtained using the molecular surfaces constructed using the atomic vdW scaled by a factor ranging from 0.5 to 2.0. This option is similar to that used by Freitag et al.

The methodology presented in this work compared with that presented by Freitag et al. presents two main differences. The first is the definition of the grid points by the use of concentric vdW grid surfaces instead of a three-dimensional Cartesian grid formed by points with a regular spacing. The second difference, and the more important, is the generation of a good initial guess (first step local fitting) to be used by a minimization procedure using an adapted downhill simplex algorithm. The original methodology proposed by Freitag et al. implemented in the GAMESS code also use a simplex algorithm, but the initial guess (or initials guesses) is defined by the user or randomly generated. For very small molecules it is possible (but not guaranteed) that the quality of the final damping parameter set will be not much affected by the initial guess choice. For larger molecules the hypersurface associated to the damping parameter set will be more complex and, as in other more complex optimization problems, it is not guaranteed that even several runs of the simplex algorithm will generate an optimal parameter set instead of nonoptimal associated to local minima of the hypersurface. The first local fitting step generates a focused initial guess based on the short distances MME damping errors and avoids the use of multiple simplex runs. The optimization methodology, including the simplex algorithm, presented in this work was implemented in a proper program outside the GAMESS code.

Results and Discussion

The corrected MME electrostatic potential, electric field intensity, and direction were compared with the ab initio values in order to test the methodology. We investigated eight small systems: H_2O (water), NH_3 (ammonia), CH_3OH (methanol), CH_2Cl_2 (dichloromethane), $(\text{CH}_3)_2\text{CO}$ (acetone), $(\text{CH}_3)_2\text{SO}$ (dimethyl sulfoxide), CH_3CN (acetonitrile), and NH_2CO (formamide) and the set of 20 amino acids. We also investigated the error in the calculation of the electrostatic interaction energy for five dimers at their standard hydrogen-bonded geometries: water–water (linear hydrogen-bonded); water–ammonia, metha-

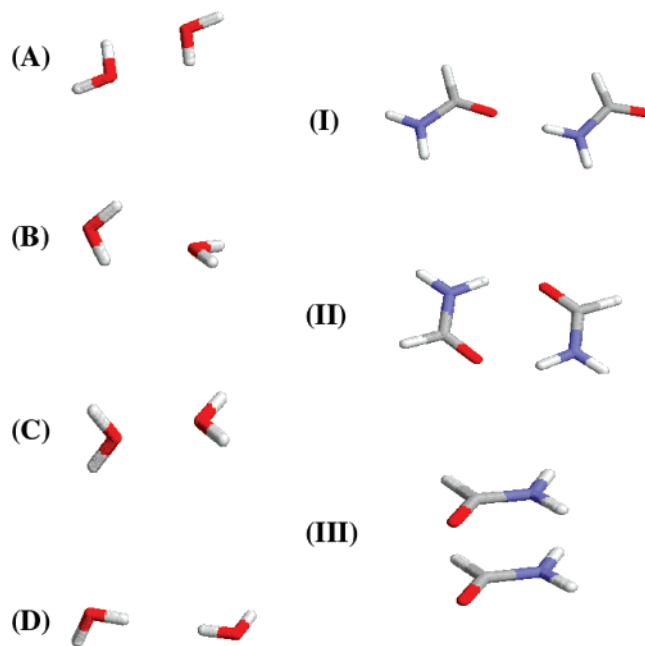


Figure 5. Four water dimer (A, B, C, and D) and three formamide (I, II, and III) dimer configurations.

nol–methanol, water–formamide (in two distinct H-bond geometries), and formamide–formamide (linear hydrogen-bonded). We also investigated the error in the calculation of the electrostatic interaction energy for the following cases: (i) cyclic (Figure 5A) and bifurcated (Figure 5B) hydrogen-bonded water–water geometries; (ii) two repulsive water–water geometries (Figure 5, parts C and D); (iii) a cyclic hydrogen-bonded formamide–formamide geometry (Figure 5II); (iv) a repulsive formamide–formamide geometry (Figure 5III). The present study of the electrostatic interaction energy was performed using eqs 3 and 4 excluding the constant nuclear–nuclear $Z_i Z_j / r_{ij}$ contribution. The small molecules geometry optimization were performed at the Hartree–Fock/6-31G** and 6-31G**+ level. The MMEs were obtained for all systems from their individual (i.e., noninteracting) optimized geometry. Our results are compared with the Morokuma procedure,³⁴ where the separation of the electronic and nuclear contribution was obtained from a modification of the algorithm implemented in the electronic structure code GAMESS.³⁷

The values obtained for the damping parameters for H_2O , NH_3 , CH_3OH , CH_2Cl_2 , $(\text{CH}_3)_2\text{CO}$, $(\text{CH}_3)_2\text{SO}$, CH_3CN , and NH_2CO using the 6-31G** and 6-31G**+ basis sets are shown in Table 1.

Electrostatic Interaction Energy Analysis. All the values for the electrostatic interaction energy of the dimers were obtained using the 6-31G** basis set. The results obtained for the electrostatic interaction energy of the dimers at their standard H-bonded geometries (see results in Figure 1A, Figure 2, and Figure 4I) show that the use of the $\{\alpha_i\}^{\text{inner}}$ parameter set gives the best results with an average absolute difference, at the equilibrium distances, of 0.26 kcal/mol between the value obtained using the corrected MME method and the value obtained using the Morokuma analysis.³⁴ At the H-bond equilibrium distances the $\{\alpha_i\}^{\text{med}}$ and the $\{\alpha_i\}^{\text{vdW}}$ parameter sets present, respectively, an average absolute difference of 0.49 and 0.89 kcal/mol. An average absolute difference of 1.00 kcal/mol was obtained using the standard MME method. When evaluating the electrostatic interaction energy error at donor–acceptor smaller distances we found that the use of the parameter set $\{\alpha_i\}^{\text{inner}}$ shows a significantly better performance than the other

TABLE 1: Values of the Calculated MME Damping Parameter Sets for the Monomer Molecules

monomer	expansion point	$\{\alpha_i\}^{\text{inner}}$ 6-31G** ^a	$\{\alpha_i\}^{\text{vdW}}$ 6-31G** ^b	$\{\alpha_i\}^{\text{med}}$ 6-31G** ^c	$\{\alpha_i\}^{\text{inner}}$ 6-31G**+ ^a	$\{\alpha_i\}^{\text{vdW}}$ 6-31G**+ ^b	$\{\alpha_i\}^{\text{med}}$ 6-31G**+ ^c	$\{\alpha_i\}^{\text{ref}}$ 6-31G**+ ^d
H ₂ O	O	3.644	4.039	3.781	3.500	3.603	3.550	3.553
	H	4.262	13.870	4.450	5.250	9.740	5.821	5.575
	O–H bm ^e	19.996	3.586	5.468	19.998	20.000	15.506	18.897
NH ₃	N	3.451	3.602	3.577	2.995	3.114	3.040	
	H	4.028	3.902	3.476	5.406	19.990	6.734	
	N–H bm	2.934	3.715	3.624	19.941	11.839	18.947	
CH ₃ OH	C	3.954	3.495	3.836	4.265	4.308	4.224	18.651
	O	3.741	4.114	3.866	3.607	3.737	3.660	3.647
	H (methyl)	3.168	3.389	3.291	3.142	3.377	3.245	3.118
	H (hydroxyl)	4.446	4.362	4.666	5.054	8.114	20.000	5.782
	C–H bm	2.755	4.451	3.160	2.660	3.004	3.009	3.080
	C–O bm	8.089	12.070	19.456	20.000	6.634	3.370	18.897
	O–H bm	20.000	7.986	6.319	10.874	10.135	5.224	18.897
CH ₂ Cl ₂	C	4.103	9.591	4.640	4.083	5.886	4.670	18.897
	Cl	3.355	3.472	3.387	3.343	3.403	3.359	3.346
	H	3.304	3.652	3.445	3.342	3.950	3.502	3.326
	C–Cl bm	19.727	2.289	14.423	19.761	11.156	14.471	18.897
	C–H bm	2.725	2.745	2.702	2.720	2.472	2.653	3.779
(CH ₃) ₂ CO	C (methyl)	11.220	4.599	10.443	10.712	8.730	3.202	3.571
	C (carboxyl)	4.033	5.634	3.988	2.462	8.820	4.578	3.307
	O	3.839	4.183	3.905	3.543	3.773	3.750	3.723
	H	3.631	5.779	3.733	3.980	2.882	3.307	3.307
	C–O bm	3.199	2.975	3.271	19.996	2.769	2.205	2.967
	C–C bm	1.761	20.000	2.400	0.416	9.230	2.038	1.946
	C–H bm	1.722	2.152	2.088	0.887	14.260	3.557	3.931
(CH ₃) ₂ SO	C (methyl)	12.228	8.982	3.821	3.711	7.187	3.978	5.499
	S	3.337	3.312	3.311	3.256	3.308	3.284	3.439
	O	3.748	4.091	3.844	3.640	3.743	3.665	3.666
	H	3.499	4.306	3.470	3.132	3.783	3.337	3.137
	S–O bm	10.044	4.804	11.248	6.035	19.998	17.491	18.897
	S–C bm	2.370	7.166	4.606	1.104	16.495	1.755	2.305
	C–H bm	1.817	2.242	2.639	2.534	2.395	2.600	2.816
CH ₃ CN	C (methyl)	12.096	3.741	4.113	3.708	4.130	4.722	4.100
	C (cyano)	3.634	5.757	3.904	3.781	8.413	4.006	3.703
	N	3.473	3.891	3.726	3.408	3.626	3.420	3.420
	H	3.728	3.863	3.449	3.366	3.882	4.080	3.326
	C–N bm	2.643	2.512	3.904	2.230	2.183	2.304	2.797
	C–C bm	4.374	13.205	20.000	12.917	20.000	20.000	1.058
	C–H bm	1.750	2.754	2.489	2.625	2.592	2.143	2.910
NH ₃ CO	O	3.769	4.230	3.896	3.651	3.829	3.702	
	C	4.134	5.754	4.131	4.251	14.195	4.951	
	N	3.182	3.376	3.218	3.085	3.169	3.094	
	H (aldehyde)	3.198	3.389	3.289	2.817	3.345	3.348	
	H (amine)	4.997	20.000	19.997	20.000	19.991	15.658	
	C–O bm	3.255	2.827	3.195	3.013	2.617	2.823	
	C–H bm	2.786	3.138	3.323	10.307	3.518	2.920	
	C–N bm	11.908	3.250	10.025	7.267	4.310	6.683	
	N–H bm	19.989	6.525	6.526	6.069	8.643	20.000	

^a Parameters obtained using the five inner concentric molecular surfaces of grid points. ^b Parameters obtained using only points at the vdW molecular surface. ^c Parameters obtained using the molecular surfaces constructed using the atomic VdW scaled by a factor ranging from 0.5 to 2.0.

^d Parameters from Freitag et al. (ref 21). ^e The abbreviation “bm” refers to bond midpoint.

parameter sets. Moreover, from Figure 2, parts C and D, it is clear that the use of the parameter set $\{\alpha_i\}^{\text{inner}}$ overestimates (positive errors) the charge penetration error for the formamide–water system at the hydrogen-bond equilibrium distance.

Inspired in the work of Piquemal et al.²² we also analyzed the performance of the three parameter sets in nonstandard water–water (geometries in Figure 5A–D, results in Figure 3) and formamide–formamide (geometries in Figure 5, parts II and III, results in Figure 4) configurations. Only for the cyclic H-bonded formamide–formamide geometry the $\{\alpha_i\}^{\text{inner}}$ parameter set clearly gives the best results (Figure 4II) for all the distances considered. For the bifurcated H-bond (Figure 3B) and O–O repulsive water–water geometries (Figure 3C) the $\{\alpha_i\}^{\text{inner}}$ parameter set is superior to the other parameter sets

only at very short O–O distances, for these configurations at O–O distances <2.4 Å and >2.0 Å the $\{\alpha_i\}^{\text{med}}$ parameter set give the best results. For the H–H repulsive water–water geometry (Figure 3D) the parameter sets $\{\alpha_i\}^{\text{inner}}$ and $\{\alpha_i\}^{\text{med}}$ have practically the same performance. Surprisingly, for the cyclic H-bond water–water configuration (results in Figure 3A) and the formamide–formamide repulsive configuration (results in Figure 4III) the best performance is achieved using the $\{\alpha_i\}^{\text{vdW}}$ parameter set and the worst using the $\{\alpha_i\}^{\text{inner}}$ parameter set. It is not clear for us a possible explanation for these results. Moreover, for these systems the results obtained using the $\{\alpha_i\}^{\text{med}}$ parameter set are better than the ones obtained using the $\{\alpha_i\}^{\text{inner}}$ parameter set even at shorter distances. Analyzing the performance of the $\{\alpha_i\}^{\text{med}}$ parameter set, at the equilibrium

TABLE 2: Monomer Molecular Electrostatic Errors at Two Molecular Surfaces Calculated from the Standard and from the Modified MME Method Using Three Different Damping Parameter Sets (6-31G Basis Set)**

		vdW surface ^a			1.2*vdW surface ^b		
		rmsd (V) ^c	rmsd (E) ^d	θ error ^e	rmsd (V)	rmsd (E)	θ error
H ₂ O	MME/ ^f	5.628	0.913	21.27	1.043	0.196	5.81
	{ α_i } ^{vdW}	0.969	0.224	5.66	0.660	0.060	1.83
	{ α_i } ^{inner}	3.086	0.212	6.70	1.539	0.174	4.19
	{ α_i } ^{med}	1.801	0.146	4.06	1.107	0.117	2.71
NH ₃	MME	8.670	1.587	30.95	2.184	0.407	15.10
	{ α_i } ^{vdW}	1.356	0.242	8.36	0.637	0.052	3.42
	{ α_i } ^{inner}	2.289	0.253	5.57	1.132	0.084	5.63
	{ α_i } ^{med}	2.643	0.312	6.48	1.421	0.150	4.03
CH ₃ OH	MME	6.121	0.948	39.37	2.006	0.255	29.38
	{ α_i } ^{vdW}	1.345	0.227	7.56	0.811	0.071	5.97
	{ α_i } ^{inner}	3.059	0.217	7.78	1.640	0.157	6.79
	{ α_i } ^{med}	1.847	0.155	6.96	1.094	0.102	5.90
CH ₂ Cl ₂	MME	7.154	0.683	70.58	1.724	0.248	24.30
	{ α_i } ^{vdW}	1.054	0.180	20.33	0.603	0.047	6.44
	{ α_i } ^{inner}	1.956	0.237	8.12	1.027	0.079	10.78
	{ α_i } ^{med}	1.450	0.195	10.99	0.837	0.057	9.08
(CH ₃) ₂ CO	MME	6.911	0.941	51.32	2.138	0.277	37.60
	{ α_i } ^{vdW}	1.427	0.399	9.38	1.158	0.076	5.91
	{ α_i } ^{inner}	7.695	0.394	10.22	5.182	0.346	10.18
	{ α_i } ^{med}	2.875	0.192	7.70	2.121	0.134	6.32
(CH ₃) ₂ SO	MME	7.342	1.034	42.17	2.289	0.297	26.12
	{ α_i } ^{vdW}	2.199	0.360	11.92	1.199	0.080	7.07
	{ α_i } ^{inner}	6.143	0.387	11.99	3.903	0.291	8.43
	{ α_i } ^{med}	2.539	0.229	11.34	1.331	0.114	7.10
CH ₃ CN	MME	8.432	1.053	47.71	2.268	0.345	15.42
	{ α_i } ^{vdW}	1.374	0.271	11.76	1.057	0.066	3.78
	{ α_i } ^{inner}	7.106	0.401	13.59	4.542	0.328	8.31
	{ α_i } ^{med}	2.661	0.214	5.69	1.798	0.123	5.15
NH ₃ CO	MME	6.829	0.981	28.41	1.749	0.261	14.46
	{ α_i } ^{vdW}	1.043	0.247	9.25	0.834	0.053	2.36
	{ α_i } ^{inner}	3.120	0.211	7.76	1.758	0.160	5.48
	{ α_i } ^{med}	2.043	0.146	6.53	1.300	0.107	4.01
all ^g	MME	7.136	1.017	41.47	1.925	0.286	21.02
	{ α_i } ^{vdW}	1.345	0.269	10.53	0.870	0.063	4.60
	{ α_i } ^{inner}	4.307	0.289	8.97	2.590	0.202	7.47
	{ α_i } ^{med}	2.232	0.199	7.47	1.376	0.11	5.54

^a Results for values calculated at the van der Waals molecular surface. ^b Results for values calculated at the 1.2*vdW molecular surface. ^c Root-mean-square deviation (rmsd) for the electrostatic potential (kcal/mol). ^d Root-mean-square deviation (rmsd) for the electric field intensity (V/Å). ^e Absolute mean absolute angular error (deg). ^f Not damped MME results. ^g Average results for all systems.

distances, for the water–water cyclic (Figure 3A) and bifurcated (Figure 3B) H-bonded configurations and for the formamide–formamide cyclic (Figure 4II) H-bonded configuration we observe errors ≤ 0.9 kcal/mol (a value close to the one obtained by Piquemal et al. using a distinct damping function and a distinct basis set). The results obtained for the dimers in standard and nonstandard geometries show that only the { α_i }^{med} parameter set gives consistently good results for all the investigated configurations and therefore is the best choice for intermolecular energy calculations using damped MMEs.

Electrostatic Potential and Electric Field Analysis. The molecular electrostatic properties, electrostatic potential, and electric field intensity and direction, were investigated at the vdW and 1.2*vdW grid point surfaces using the 6-31G** (Table 2) and the 6-31G**+ (Table 3) LCAO basis sets.

For all studied monomer molecules and for both basis sets we obtained more accurate results using the damping parameter set { α_i }^{vdW}. Table 2 shows calculated errors, using 6-31G**, at the molecular vdW surface and at the 1.2*vdW surface for the parameters: (i) { α_i }^{vdW}—an average error decrease of 81.4% at the vdW surface (54.8%) for the electrostatic potential, 73.6% (77.9%) for the electric field intensity, and 74.6% (78.1%) for the electric field mean absolute angular error; (ii) { α_i }^{inner}—an

average error decrease of 39.6% (−34.6%) for the electrostatic potential, 71.6% (29.2%) for the electric field intensity, and 78.4% (64.5%) for the electric field mean absolute angular error; (iii) { α_i }^{med}—an average error decrease of 68.7% (28.5%) for the electrostatic potential, 80.5% (60.5%) for the electric field intensity, and 82.0% (73.7%) for the electric field mean absolute angular error. The values given in parentheses relate to the 1.2*vdW surface and a negative value stand for error increase. Table 3 shows calculated errors, using 6-31G**+, at the molecular vdW surface and at the 1.2*vdW surface: (i) { α_i }^{vdW}—an average error decrease of 71.1% (57.4%) for the electrostatic potential, 70.2% (71.3%) for the electric field intensity, and 67.5% (67.1%) for the electric field mean absolute angular error; (ii) { α_i }^{inner}—an average error decrease of 51.1% (4.1%) for the electrostatic potential, 65.2% (46.0%) for the electric field intensity, and 71.5% (64.9%) for the electric field mean absolute angular error; (iii) { α_i }^{med}—an average error decrease of 67.7% (49.7%) for the electrostatic potential, 73.3% (68.5%) for the electric field intensity, and 72.0% (67.7%) for the electric field mean absolute angular error.

The improvements observed using the parameters { α_i }^{vdW} are more pronounced for electrostatic potential calculations. For the electric field intensity and direction the { α_i }^{med}

TABLE 3: Monomer Molecular Electrostatic Errors at Two Molecular Surfaces Calculated from the Standard MME and from the Modified MME Method Using Three Different Damping Parameter Sets (6-31G+ Basis Set)**

		vdW surface ^a			1.2*vdW surface ^b		
		rmsd (V) ^c	rmsd (E) ^d	θ error ^e	rmsd (V)	rmsd (E)	θ error
H ₂ O	MME ^f	8.845	1.230	26.37	2.262	0.369	8.22
	$\{\alpha_i\}^{\text{vdW}}$	1.862	0.261	7.58	0.695	0.081	2.66
	$\{\alpha_i\}^{\text{inner}}$	2.375	0.250	7.93	1.020	0.105	3.65
	$\{\alpha_i\}^{\text{med}}$	2.003	0.246	7.39	0.833	0.089	3.05
	$\{\alpha_i\}^{\text{ref } g}$	1.996	0.247	7.38	0.826	0.089	3.04
NH ₃	MME	9.375	1.156	33.80	3.046	0.436	18.49
	$\{\alpha_i\}^{\text{vdW}}$	3.159	0.429	13.88	0.973	0.130	7.86
	$\{\alpha_i\}^{\text{inner}}$	3.760	0.403	12.34	1.202	0.102	7.59
	$\{\alpha_i\}^{\text{med}}$	3.356	0.402	12.91	1.045	0.107	7.58
	$\{\alpha_i\}^{\text{ref}}$						
CH ₃ OH	MME	7.324	1.133	37.76	2.390	0.340	26.91
	$\{\alpha_i\}^{\text{vdW}}$	1.714	0.265	7.70	0.820	0.074	5.59
	$\{\alpha_i\}^{\text{inner}}$	2.903	0.263	7.73	1.500	0.124	6.55
	$\{\alpha_i\}^{\text{med}}$	1.967	0.224	7.54	0.994	0.076	5.68
	$\{\alpha_i\}^{\text{ref}}$	2.013	0.238	7.76	1.084	0.088	5.77
CH ₂ Cl ₂	MME	7.840	0.678	71.84	1.990	0.265	27.34
	$\{\alpha_i\}^{\text{vdW}}$	1.070	0.199	16.47	0.501	0.044	5.88
	$\{\alpha_i\}^{\text{inner}}$	1.593	0.239	9.44	0.768	0.072	7.49
	$\{\alpha_i\}^{\text{med}}$	1.277	0.210	11.27	0.640	0.055	6.77
	$\{\alpha_i\}^{\text{ref}}$	1.356	0.241	10.15	0.645	0.065	7.34
(CH ₃) ₂ CO	MME	9.759	1.021	56.92	3.699	0.347	43.83
	$\{\alpha_i\}^{\text{vdW}}$	6.127	0.504	30.62	3.058	0.219	21.67
	$\{\alpha_i\}^{\text{inner}}$	13.696	0.976	22.72	11.142	0.692	18.31
	$\{\alpha_i\}^{\text{med}}$	5.913	0.485	22.13	2.994	0.214	18.93
	$\{\alpha_i\}^{\text{ref}}$	6.276	0.508	28.15	2.976	0.200	23.65
(CH ₃) ₂ SO	MME	8.814	1.246	41.58	2.841	0.401	23.57
	$\{\alpha_i\}^{\text{vdW}}$	3.418	0.423	15.71	1.425	0.132	8.86
	$\{\alpha_i\}^{\text{inner}}$	4.271	0.343	17.11	2.021	0.155	11.17
	$\{\alpha_i\}^{\text{med}}$	3.546	0.337	16.02	1.522	0.131	9.24
	$\{\alpha_i\}^{\text{ref}}$	3.639	0.349	17.50	1.540	0.141	9.93
CH ₂ CN	MME	10.077	1.095	50.35	3.066	0.396	17.85
	$\{\alpha_i\}^{\text{vdW}}$	1.502	0.271	9.85	1.128	0.071	3.85
	$\{\alpha_i\}^{\text{inner}}$	3.481	0.252	11.49	2.005	0.161	5.97
	$\{\alpha_i\}^{\text{med}}$	2.832	0.177	10.26	1.979	0.132	4.54
	$\{\alpha_i\}^{\text{ref}}$	1.907	0.233	9.63	0.941	0.091	4.65
NH ₂ CO	MME	9.197	1.145	32.03	2.765	0.363	16.71
	$\{\alpha_i\}^{\text{vdW}}$	1.717	0.239	12.00	0.792	0.086	3.72
	$\{\alpha_i\}^{\text{inner}}$	2.778	0.305	11.01	1.504	0.163	3.39
	$\{\alpha_i\}^{\text{med}}$	2.109	0.243	10.65	1.078	0.114	3.21
	$\{\alpha_i\}^{\text{ref}}$						
all ^h	MME	8.904	1.088	43.83	2.757	0.365	22.86
	$\{\alpha_i\}^{\text{vdW}}$	2.571	0.324	14.22	1.174	0.105	7.51
	$\{\alpha_i\}^{\text{inner}}$	4.357	0.379	12.47	2.645	0.197	8.01
	$\{\alpha_i\}^{\text{med}}$	2.875	0.290	12.27	1.385	0.115	7.37
	$\{\alpha_i\}^{\text{ref}}$	2.864	0.303	13.43	1.335	0.112	9.06

^a Results for values calculated at the van der Waals molecular surface. ^b Results for values calculated at the 1.2*vdW molecular surface. ^c Root-mean-square deviation (rmsd) for the electrostatic potential (kcal/mol). ^d Root-mean-square deviation (rmsd) for the electric field intensity (V/Å). ^e Absolute mean absolute angular error (deg). ^f Not damped MME results. ^g $\{\alpha_i\}^{\text{ref}}$ parameters from Freitag et al. (ref 21). ^h Average results for all systems.

parameter set shows slightly better results than the $\{\alpha_i\}^{\text{vdW}}$ parameter set at the vdW molecular surface but not at the 1.2*vdW surface. The results, at the vdW and 1.2*vdW surfaces, obtained using the $\{\alpha_i\}^{\text{inner}}$ parameter set are the worst ones. However, as expected, results obtained at the inner shells inside the vdW molecular envelope are consistently better when the set $\{\alpha_i\}^{\text{inner}}$ is used as damping parameters (only the results for the water molecule are shown in Figure 1B–D).

Analyzing the performance of the $\{\alpha_i\}^{\text{vdW}}$ damping parameters for the two distinct LCAO basis sets we observed (see Tables 2 and 3) that the percent average error decrease is practically the same for both basis. The inclusion of diffuse sp (L) shell for heavy atoms in the 6-31G**+ basis set lead to uncorrected electrostatic potential errors >1.8 kcal/mol at the vdW surface (>0.8 kcal/mol at the 1.2*vdW surface) in relation to the results obtained using the 6-31G** basis set. With the

use of the $\{\alpha_i\}^{\text{vdW}}$ damping parameters the corrected electrostatic potential errors decrease to 1.2 kcal/mol at the vdW surface (0.3 kcal/mol at the 1.2*vdW surface) in relation to the results obtained using the 6-31G** basis set showing the importance of a damping correction when using more elaborate LCAO basis sets. The results (see Table 3) obtained when using the damping parameters from Freitag et al.²¹ are practically equivalent with the ones obtained using the $\{\alpha_i\}^{\text{med}}$ damping parameters derived in this work, reflecting the similar choice in the grid points definition.

To investigate if our methodology is applicable to bigger molecules, we investigate the electrostatic properties of the 20 amino acids in two or three different conformations, most of them obtained from the crystal structures of papain (PDB ID: 1POP) and cruzipain (PDB ID: 1AIM). In this study not only the amino acid side chain were considered but also their peptide junctions. In this way each amino acid has the structure COH–

TABLE 4: Amino Acids Molecular Electrostatic Errors at Two Molecular Surfaces Calculated from the Standard and the Modified MME Method Using Three Different Damping Parameter Sets (6-31G Basis Set)**

amino acid ^a	damping parameters	vdW surface			1.2*vdW surface		
		rmsd (V) ^b	rmsd (E) ^c	θ error ^d	rmsd (V)	rmsd (E)	θ error
Ala	α -vdW	1.025 (80.9%)	0.210 (75.8%)	9.67 (72.2%)	0.742 (42.3%)	0.048 (77.1%)	4.07 (79.4%)
	α -inner	3.841 (28.4%)	0.232 (73.2%)	7.61 (78.1%)	2.177 (−69.4%)	0.177 (14.1%)	8.79 (55.3%)
	α -med	1.985 (63.0%)	0.120 (86.1%)	5.99 (82.7%)	1.288 (−0.2%)	0.105 (49.4%)	5.55 (71.8%)
Arg	α -vdW	1.195 (75.8%)	0.198 (73.2%)	11.10 (57.8%)	0.714 (40.8%)	0.055 (70.7%)	2.98 (72.3%)
	α -inner	3.384 (31.3%)	0.224 (69.6%)	6.97 (73.4%)	1.927 (−59.9%)	0.154 (18.1%)	5.77 (48.0%)
	α -med	1.844 (62.6%)	0.134 (81.8%)	5.37 (79.6%)	1.160 (3.8%)	0.092 (51.1%)	3.83 (65.4%)
Asn	α -vdW	0.930 (82.6%)	0.210 (76.6%)	8.50 (67.5%)	0.684 (43.7%)	0.047 (77.3%)	2.59 (77.9%)
	α -inner	3.287 (38.6%)	0.217 (75.8%)	6.73 (74.2%)	1.849 (−52.0%)	0.162 (20.9%)	6.85 (42.0%)
	α -med	1.897 (64.6%)	0.134 (85.0%)	5.40 (79.3%)	1.204 (0.9%)	0.105 (48.8%)	4.49 (61.9%)
Asp	α -vdW	1.134 (81.1%)	0.272 (76.1%)	8.63 (69.3%)	0.774 (43.9%)	0.059 (77.0%)	3.52 (72.1%)
	α -inner	3.766 (37.2%)	0.257 (77.5%)	7.05 (74.9%)	2.118 (−53.5%)	0.202 (21.3%)	8.86 (30.8%)
	α -med	2.187 (63.5%)	0.150 (86.8%)	5.63 (80.0%)	1.403 (−1.7%)	0.134 (47.7%)	4.92 (61.5%)
Cys	α -vdW	1.859 (71.5%)	0.345 (63.1%)	12.22 (61.2%)	0.881 (48.9%)	0.081 (67.8%)	5.73 (60.0%)
	α -inner	2.831 (56.6%)	0.286 (69.3%)	10.43 (66.9%)	1.448 (16.2%)	0.153 (38.7%)	8.39 (41.3%)
	α -med	2.257 (65.3%)	0.232 (75.1%)	9.64 (69.3%)	1.223 (28.9%)	0.109 (56.3%)	6.69 (53.2%)
Gln	α -vdW	1.052 (80.1%)	0.223 (75.3%)	9.69 (63.2%)	0.747 (41.0%)	0.050 (76.6%)	3.15 (74.2%)
	α -inner	3.494 (33.9%)	0.223 (75.4%)	6.94 (73.7%)	1.972 (−56.0%)	0.165 (23.1%)	7.25 (40.5%)
	α -med	1.957 (63.0%)	0.132 (85.4%)	5.51 (79.1%)	1.250 (1.1%)	0.103 (51.9%)	4.71 (61.3%)
Glu	α -vdW	1.110 (81.2%)	0.269 (75.6%)	8.29 (72.5%)	0.816 (42.3%)	0.056 (77.5%)	3.32 (77.5%)
	α -inner	3.891 (34.0%)	0.250 (77.3%)	7.90 (73.5%)	2.239 (−58.6%)	0.197 (20.9%)	10.81 (27.8%)
	α -med	2.172 (63.1%)	0.146 (86.7%)	5.76 (80.8%)	1.426 (−1.0%)	0.131 (47.4%)	5.69 (62.0%)
Gly	α -vdW	0.992 (82.3%)	0.215 (76.6%)	9.27 (65.9%)	0.755 (41.8%)	0.053 (75.8%)	2.60 (78.6%)
	α -inner	2.953 (47.4%)	0.213 (76.9%)	6.40 (76.4%)	1.696 (−30.8%)	0.162 (26.0%)	6.41 (47.2%)
	α -med	1.906 (66.0%)	0.135 (85.3%)	5.92 (78.2%)	1.254 (3.3%)	0.111 (49.3%)	4.86 (60.0%)
His	α -vdW	1.244 (75.9%)	0.205 (74.0%)	11.39 (62.7%)	0.815 (35.4%)	0.054 (71.1%)	4.33 (67.3%)
	α -inner	3.001 (42.2%)	0.211 (73.2%)	7.49 (75.5%)	1.666 (−31.4%)	0.142 (24.6%)	8.66 (35.4%)
	α -med	1.867 (64.4%)	0.144 (82.1%)	7.11 (76.1%)	1.151 (10.6%)	0.099 (48.1%)	5.72 (55.5%)
Ile	α -vdW	1.100 (79.5%)	0.225 (71.4%)	11.76 (74.5%)	0.775 (44.7%)	0.049 (75.5%)	8.76 (68.5%)
	α -inner	3.349 (37.1%)	0.321 (59.2%)	10.42 (77.4%)	2.678 (−91.2%)	0.220 (−9.7%)	15.06 (45.8%)
	α -med	1.942 (63.7%)	0.126 (84.0%)	7.59 (83.5%)	1.294 (7.6%)	0.100 (50.3%)	9.33 (66.4%)
Leu	α -vdW	1.122 (79.3%)	0.230 (70.2%)	13.74 (71.3%)	0.774 (45.4%)	0.053 (73.0%)	10.47 (63.5%)
	α -inner	3.888 (28.2%)	0.233 (69.8%)	9.25 (80.7%)	2.284 (−61.1%)	0.170 (13.8%)	17.12 (40.3%)
	α -med	1.952 (63.9%)	0.124 (84.0%)	7.73 (83.9%)	1.321 (6.8%)	0.098 (50.2%)	12.61 (56.0%)
Lys	α -vdW	0.999 (78.9%)	0.196 (74.5%)	7.36 (67.8%)	0.678 (45.4%)	0.047 (75.3%)	2.51 (74.8%)
	α -inner	3.745 (20.7%)	0.240 (68.7%)	6.68 (70.8%)	2.209 (−78.1%)	0.184 (3.8%)	5.77 (42.0%)
	α -med	1.734 (63.3%)	0.119 (84.5%)	4.94 (78.4%)	1.134 (8.6%)	0.095 (50.6%)	3.60 (63.8%)
Met	α -vdW	1.603 (73.3%)	0.272 (68.5%)	11.10 (68.9%)	0.890 (45.5%)	0.070 (69.0%)	6.26 (67.5%)
	α -inner	3.349 (44.3%)	0.360 (58.4%)	9.44 (73.6%)	2.407 (−47.8%)	0.213 (5.2%)	9.96 (48.1%)
	α -med	2.053 (65.7%)	0.208 (75.9%)	7.51 (78.9%)	1.178 (28.0%)	0.113 (49.9%)	7.24 (62.4%)
Phe	α -vdW	1.037 (80.7%)	0.188 (74.5%)	14.40 (67.1%)	0.704 (47.3%)	0.044 (76.9%)	5.89 (65.8%)
	α -inner	2.884 (46.2%)	0.210 (71.5%)	8.95 (79.6%)	1.631 (−22.3%)	0.136 (28.6%)	11.76 (31.6%)
	α -med	1.766 (67.1%)	0.142 (80.7%)	8.70 (80.1%)	1.132 (15.1%)	0.089 (53.3%)	8.92 (48.1%)
Pro	α -vdW	1.058 (79.5%)	0.224 (74.4%)	9.26 (73.6%)	0.696 (46.8%)	0.049 (78.2%)	4.32 (73.4%)
	α -inner	3.596 (30.3%)	0.355 (59.3%)	8.97 (74.4%)	3.507 (−169.1%)	0.237 (−6.0%)	9.97 (39.0%)
	α -med	2.038 (60.5%)	0.150 (82.8%)	6.16 (82.5%)	1.237 (5.5%)	0.106 (53.0%)	5.67 (65.0%)
Ser	α -vdW	1.009 (80.9%)	0.212 (76.1%)	7.86 (68.7%)	0.712 (44.1%)	0.050 (75.9%)	2.74 (74.6%)
	α -inner	3.256 (38.3%)	0.210 (76.3%)	6.96 (72.2%)	1.811 (−42.2%)	0.160 (22.2%)	6.72 (38.4%)
	α -med	1.889 (64.1%)	0.127 (85.6%)	5.51 (78.0%)	1.186 (6.8%)	0.103 (49.7%)	4.35 (59.8%)
Thr	α -vdW	1.004 (80.8%)	0.223 (73.7%)	8.14 (74.8%)	0.722 (44.4%)	0.050 (75.0%)	3.86 (78.0%)
	α -inner	3.669 (30.0%)	0.218 (74.3%)	7.96 (75.2%)	2.088 (−60.6%)	0.168 (15.7%)	8.81 (49.7%)
	α -med	1.948 (62.8%)	0.128 (84.9%)	5.76 (82.1%)	1.247 (4.1%)	0.103 (48.1%)	5.62 (67.9%)
Trp	α -vdW	1.298 (76.2%)	0.212 (70.7%)	23.22 (49.8%)	0.938 (30.2%)	0.052 (72.8%)	7.06 (59.3%)
	α -inner	3.324 (39.1%)	0.231 (68.1%)	10.83 (76.6%)	1.907 (−41.8%)	0.142 (25.0%)	13.12 (24.5%)
	α -med	1.989 (63.5%)	0.160 (78.0%)	11.78 (74.5%)	1.257 (6.6%)	0.093 (51.0%)	9.26 (46.7%)
Tyr	α -vdW	1.117 (79.1%)	0.217 (72.4%)	8.85 (53.2%)	0.819 (36.5%)	0.047 (76.7%)	5.39 (67.0%)
	α -inner	2.964 (44.4%)	0.208 (73.5%)	8.09 (79.9%)	1.676 (−30.2%)	0.136 (32.6%)	11.36 (30.4%)
	α -med	1.872 (64.9%)	0.144 (81.7%)	8.86 (78.0%)	1.187 (7.8%)	0.090 (55.6%)	8.05 (50.7%)
Val	α -vdW	0.979 (81.6%)	0.220 (72.7%)	10.07 (76.8%)	0.720 (46.7%)	0.045 (77.5%)	7.60 (71.3%)
	α -inner	3.930 (26.0%)	0.234 (71.0%)	8.29 (80.9%)	2.283 (−69.0%)	0.178 (11.8%)	13.09 (50.5%)
	α -med	1.878 (64.6%)	0.120 (85.1%)	6.89 (84.2%)	1.239 (8.3%)	0.097 (51.7%)	9.01 (65.9%)
all ^e	MME	5.412	0.855	33.94	1.339	0.209	16.35
	α -vdW	1.167 (78.4%)	0.236 (72.3%)	11.41 (66.3%)	0.816 (38.6%)	0.058 (71.9%)	4.98 (69.4%)
	α -inner	3.428 (36.4%)	0.243 (71.3%)	8.18 (75.1%)	2.058 (−54.62%)	0.171 (17.9%)	9.75 (39.8%)
	α -med	1.949 (64.0%)	0.142 (83.2%)	6.88 (79.5%)	1.237 (7.1%)	0.103 (50.6%)	6.53 (59.9%)

^a Mean values calculated from two/three distinct amino acids conformations. ^b Root-mean-square deviation (rmsd) for the electrostatic potential (kcal/mol). ^c Root-mean-square deviation (rmsd) for the electric field intensity (V/Å). ^d Absolute mean absolute angular error (deg). ^e Average results for all systems. The values of the error decrease in percent are put in brackets (negative values stand for error increase).

NH—CR—CO—NH₂, where R is the respective amino acid side chain, which is the molecular fragment used in the protein OME

reassociation method.¹⁷ Original crystallographic coordinates were used for the calculations without modification; only the

TABLE 5: Amino Acids Molecular Electrostatic Errors at Two Molecular Surfaces Calculated (6-31G Basis Set) with Different Damping Parameters for the Backbone and Side-Chain Expansion Points**

amino acid	vdW surface			1.2*vdW surface		
	rmsd (V) ^a	rmsd (E) ^b	θ error ^c	rmsd (V)	rmsd (E)	θ error
Gly(o)	1.906 (66.0%)	0.135 (85.3%)	5.92 (78.2%)	1.254 (3.3%)	0.111 (49.3%)	4.86 (60.0%)
Gly(1)	2.276 (59.4%)	0.166 (82.0%)	5.74 (78.9%)	1.415 (−9.1%)	0.133 (39.3%)	5.22 (57.0%)
Asn(o) ^d	1.897 (64.6%)	0.134 (85.0%)	5.40 (79.3%)	1.204 (0.9%)	0.105 (48.8%)	4.49 (61.9%)
Asn(1) ^d	2.240 (58.2%)	0.152 (83.1%)	5.58 (78.6%)	1.333 (−9.6%)	0.118 (42.4%)	5.34 (54.6%)
Asn(2) ^d	1.972 (63.2%)	0.140 (84.4%)	5.42 (79.3%)	1.234 (−1.5%)	0.109 (47.0%)	4.60 (60.9%)
Ser(o) ^d	1.889 (64.1%)	0.127 (85.6%)	5.51 (78.0%)	1.186 (6.8%)	0.103 (49.7%)	4.35 (59.8%)
Ser(1) ^d	1.866 (64.6%)	0.134 (84.9%)	5.66 (77.4%)	1.162 (8.7%)	0.104 (49.2%)	4.23 (60.9%)

^a Root-mean-square deviation (rmsd) for the electrostatic potential (kcal/mol). ^b Root-mean-square deviation (rmsd) for the electric field intensity (V/Å). ^c Absolute mean absolute angular error (degrees). The values of the error decrease in percent are put in brackets (negative values stand for error increase). (o) Values obtained using the original damping parameters (see Table 4); Gly(1) values obtained using damping parameters from formamide; Asn(1) values obtained using the Gly damping parameters for the backbone and the formamide damping parameters for the lateral chain; Asn(2) values obtained using the Gly damping parameters for the backbone and for the lateral chain; Ser(1) values obtained using the Gly damping parameters for the backbone and the methanol damping parameters for the lateral chain. ^d Mean values calculated from three distinct amino acids conformations.

lacking hydrogens were added with standard geometries. The amino acids conformations used in this work are given in the Supporting Information.

The results obtained for the 20 amino acids are shown in Table 4 and are of the same quality as those obtained for the smaller molecules (Table 2). The damping parameter set $\{\alpha_i\}^{\text{vdW}}$ performs better than the other sets for the electrostatic potential at both molecular surfaces and also for the electric field (intensity and direction) at the 1.2*vdW surface. The $\{\alpha_i\}^{\text{med}}$ set performs better than the $\{\alpha_i\}^{\text{vdW}}$ set only for the electric field at the vdW surface. The results obtained for the electrostatic potential at the 1.2*vdW molecular surface with the set $\{\alpha_i\}^{\text{inner}}$ are worse than those obtained using the standard MME method (a mean error increase of 54.2%). It is interesting to note that the Cys and Met amino acids are the ones with the bigger errors for all electrostatic properties calculated at the vdW molecular surface. These two amino acids are the only ones with a sulfur atom, and probably this result indicates that the functional form of the damping function used have to be improved for this type of atom. The values obtained for the damping parameters for the 20 amino acids are given in the Supporting Information.

Investigating the obtained set of damping parameters we observe that they differ for all amino acids even for similar atomic groups. Two important questions for future simulations involving proteins are “a new set of values have to be determined for every new amino acid fragment?” and “can we construct a more conformationally insensitive amino acid set of damping parameters based on the ones obtained for the small fragments (e.g., formamide and methanol)?”. In order to answer these questions we made a comparative analysis, using the $\{\alpha_i\}^{\text{med}}$ parameter set, for three amino acids: glycine as a model for the protein backbone, asparagine, and serine (results shown in Table 5). For glycine the results obtained using the original damping parameters were compared with the ones obtained replacing the terminal damping parameters (NH₂ and HC=O terminal groups) by the formamide equivalent ones (Gly case 1). For asparagine the results obtained using the original damping parameters were compared with the ones obtained replacing the backbone damping parameters by the equivalent glycine ones and the side-chain (C=ONH₂) parameters replaced by the formamide equivalent ones (Asn case 1). For asparagine we also compared the original results with the ones obtained replacing the backbone and the side-chain (C=ONH₂) damping parameters by the equivalent glycine ones (Asn case 2). For serine we compared the original results with the ones obtained replacing the backbone damping parameters by the equivalent

glycine ones and the side-chain (CH₃OH) parameters replaced by the methanol equivalent ones (Ser case 1). Inspecting the results shown in Table 5 we arrived to the following conclusions: (i) The better choice is to maintain the original glycine damping parameters to describe the protein backbone instead of using the formamide equivalent ones. Calculations for all amino acids (results not shown) using these original glycine damping parameters replacing all residues backbone parameters showed that the original glycine parameters present a good transferability. (ii) For the asparagine amino acid the better choice for the side-chain damping parameters is to use the equivalent glycine parameters. (iii) Surprisingly, for serine the combination of glycine parameters for the backbone and methanol damping parameters for the side chain give better results than the original ones.

In order to obtain a more robust and general set of $\{\alpha_i\}^{\text{med}}$ damping parameters for all amino acids we tried to combine the original $\{\alpha_i\}^{\text{med}}$ set obtained for the small fragments (see Table 1, 6-31G** LCAO basis set) and the original $\{\alpha_i\}^{\text{med}}$ damping parameters obtained for the amino acids (see the Supporting Information). We called the new set of parameters $\{\alpha_i\}^{\text{med*}}$. The new set was tested for electrostatic potential and electric field (intensity and direction) calculations at the vdW molecular surface and at the 1.2*vdW surface. The rules for the construction of the new $\{\alpha_i\}^{\text{med*}}$ damping set are as follows:

(1) The original glycine damping parameters are used for all damping parameters associated to the residues backbone.

(2) The original alanine carbon sp³ damping parameters are used for some sp³ carbon atoms of Arg (CB, CG, CD), Asn (CB), Gln (CB, CG), Glu (CB), His (CB), Ile (all carbons), Leu (all carbons), Lys (CB, CG, CD), Met (CB, CG, CE), Phe (CB), Thr (CG), Trp (CB), Tyr (CB), Val (all carbons).

(3) For the side chains (C=ONH₂ group) of asparagine and glutamine we used the original equivalent damping parameters of glycine.

(4) For the side chain CH₃OH groups of serine, threonine, and tyrosine we used the original equivalent damping parameters of methanol.

(5) For the side chains of Asp and Glu COO[−] acid groups we used the original equivalent damping parameters of the aspartic acid.

(6) For the aromatic group of phenylalanine and tyrosine we used the original equivalent damping parameters of the phenylalanine aromatic group.

(7) For the other chemical groups not mentioned above we used the original $\{\alpha_i\}^{\text{med}}$ damping parameters described in the Supporting Information.

TABLE 6: Amino Acids Molecular Electrostatic Errors at Two Molecular Surfaces Calculated (6-31G Basis Set) with the Modified $\{\alpha_i\}^{\text{med}*}$ Damping Parameter Sets**

amino acid ^a	vdW surface			1.2*vdW surface		
	rmsd (V) ^b	Rmsd (E) ^c	θ error ^d	rmsd (V)	rmsd (E)	θ error
Ala	2.000 (62.7%)	0.126 (85.5%)	6.30 (81.9%)	1.276 (0.7%)	0.107 (48.0%)	5.42 (72.4%)
Arg	2.062 (58.2%)	0.142 (80.7%)	5.66 (78.5%)	1.267 (−5.1%)	0.102 (45.8%)	3.98 (64.1%)
Asn	1.972 (63.2%)	0.140 (84.4%)	5.42 (79.3%)	1.234 (−1.5%)	0.109 (47.0%)	4.60 (60.9%)
Asp	2.122 (64.6%)	0.154 (86.5%)	5.88 (79.1%)	1.348 (2.2%)	0.136 (47.1%)	4.48 (64.9%)
Cys	2.296 (64.7%)	0.234 (74.9%)	9.77 (69.0%)	1.236 (28.2%)	0.113 (54.9%)	6.73 (53.0%)
Gln	2.035 (61.5%)	0.136 (84.9%)	5.81 (78.0%)	1.275 (−0.8%)	0.106 (50.5%)	4.71 (61.3%)
Glu	2.139 (63.7%)	0.151 (86.3%)	5.93 (80.2%)	1.379 (2.3%)	0.133 (46.6%)	5.14 (65.5%)
Gly	1.906 (66.0%)	0.135 (85.3%)	5.92 (78.2%)	1.254 (3.3%)	0.111 (49.3%)	4.86 (60.0%)
His	1.934 (63.1%)	0.152 (81.2%)	7.89 (73.7%)	1.207 (6.0%)	0.098 (46.7%)	5.67 (56.0%)
Ile	1.954 (63.5%)	0.131 (83.4%)	8.05 (82.5%)	1.276 (8.9%)	0.103 (48.5%)	9.15 (67.0%)
Leu	1.884 (65.2%)	0.129 (83.2%)	8.21 (82.9%)	1.253 (11.5%)	0.100 (49.3%)	11.78 (58.9%)
Lys	1.813 (61.6%)	0.124 (83.8%)	5.19 (77.4%)	1.160 (6.5%)	0.098 (48.7%)	3.58 (63.9%)
Met	2.287 (61.8%)	0.213 (75.3%)	7.54 (78.9%)	1.353 (17.1%)	0.115 (48.5%)	7.61 (60.6%)
Phe	1.815 (66.2%)	0.145 (80.4%)	8.68 (80.2%)	1.151 (13.7%)	0.093 (51.2%)	9.24 (46.4%)
Pro	2.056 (60.2%)	0.147 (83.1%)	7.04 (80.0%)	1.278 (2.3%)	0.103 (54.4%)	5.38 (66.8%)
Ser	1.866 (64.6%)	0.134 (84.9%)	5.66 (77.4%)	1.162 (8.7%)	0.104 (49.2%)	4.23 (60.9%)
Thr	1.921 (63.3%)	0.137 (83.8%)	6.10 (81.0%)	1.216 (6.5%)	0.105 (47.1%)	5.38 (69.3%)
Trp	2.025 (62.9%)	0.161 (77.8%)	11.62 (74.8%)	1.262 (6.3%)	0.093 (50.7%)	9.75 (43.9%)
Tyr	1.847 (65.4%)	0.142 (81.9%)	10.85 (73.0%)	1.158 (10.1%)	0.091 (55.1%)	7.21 (55.8%)
Val	1.962 (63.1%)	0.126 (84.4%)	7.14 (83.6%)	1.284 (5.0%)	0.102 (49.3%)	8.91 (66.3%)
all ^e						
α -med*	1.986 (63.2%)	0.146 (82.7%)	7.23 (78.5%)	1.248 (6.3%)	0.106 (49.4%)	6.40 (60.7%)
α -med ^f	1.949 (64.0%)	0.142 (83.2%)	6.88 (79.5%)	1.237 (7.1%)	0.103 (50.6%)	6.53 (59.9%)

^a Mean values calculated from two or three distinct amino acids conformations. ^b Root-mean-square deviation (rmsd) for the electrostatic potential (kcal/mol). ^c Root-mean-square deviation (rmsd) for the electric field intensity (V/Å). ^d Absolute mean absolute angular error (deg). ^e Average results for all systems. The values of the error decrease in percent are put in brackets (negative values stand for error increase). ^f Original results from Table 4.

In Table 6 we show the results obtained using the new $\{\alpha_i\}^{\text{med}*}$ damping set. For each amino acid we present the mean values relative to calculations using the same damping set parameter on different conformations and their respective MMEs. Surprisingly, we observe that the damping parameter set $\{\alpha_i\}^{\text{med}*}$ has a very good global performance with results very close to the ones obtained using the original $\{\alpha_i\}^{\text{med}}$ damping sets calculated for each specific amino acid conformation. Moreover, for some amino acids (i.e., Ala, Asp, Glu, Ile, Leu, Ser, Thr, and Tyr) the mean performance, at one or both vdW surfaces, is better than the one shown in Table 4. These results indicate that the new constructed amino acid $\{\alpha_i\}^{\text{med}*}$ damping set can be to a certain extent more insensitive to protein backbone and residue side-chain conformational changes. We can also conclude that, at least for the amino acid residues, the damping parameters obtained for specific chemical groups have a certain degree of transferability.

Conclusions

In this work we presented a general two-step local fitting procedure, based on the methodology proposed by Freitag et al.,²¹ to optimize the parameters of exponential damping functions to account for charge penetration effects in the MMEs method. The principal aspect of the proposed methodology is a first local fitting step which generates a focused initial guess to improve the performance of a simplex method (avoiding the use of multiple runs and the choice of initial guesses). We investigated the error in the calculation of the electrostatic interaction energy for five dimers (in standard and nonstandard configurations) and also the error in deriving electrostatic molecular properties (potential and electric field) of eight small molecular systems and for the 20 amino acids set. Moreover, we tested and analyzed three distinct ways to obtain optimized damping parameters sets. Our results show that the methodology performs well not only for small molecules but also for relatively

larger molecular systems. The two-step local fitting procedure has a reasonable computational cost and always converges to a good set of damping parameters (regardless of the number of expansion centers). Another advantage of the method is its independence with respect to the type of the ab initio electronic structure quantum calculation used to derive the MMEs. In particular, the damping parameter set $\{\alpha_i\}^{\text{med}}$ is more appropriate for electrostatic interaction energy calculations using effective fragment models for modeling solvent effects in quantum mechanical calculations.¹³ This result corroborate the grid point definition made by Freitag et al. The set $\{\alpha_i\}^{\text{vdW}}$ is more appropriate for the calculation of molecular electrostatic properties of small systems and also for larger ones (e.g., protein macromolecules) by fragment reassociation methods^{17,18,20} at distances greater or equal to the vdW radii.

The present approach can be a very useful tool to parametrize electrostatic damping functions, and its features permit a systematic and automatic use in a broad class of molecular studies using the MME method. We also expect that the present methodology can be adapted to optimize the parameters of improved functional forms for the damping function²² with more than one parameter associated for each expansion center.

We also investigated the possibility to construct a more robust and general $\{\alpha_i\}^{\text{med}}$ amino acid damping parameter set using the original damping parameters derived for the small fragments (e.g., methanol, formamide) and for the amino acids. We arrived to construct a damping parameter set, called $\{\alpha_i\}^{\text{med}*}$, more insensitive to protein backbone and residue side-chain conformational changes. This new damping set has a very good global performance obtaining results very close to the ones obtained with the original $\{\alpha_i\}^{\text{med}}$ amino acids damping sets calculated for each specific amino acid conformation. This result is important for future protein simulations using ab initio based polarizable classical methods. In this sense, this new amino acid damping set can be very useful to permit these methods to be

more easily applicable in the following types of biomolecular studies: (i) to reevaluate the intermolecular energy of protein–ligand binding conformations obtained from docking methods;³⁸ (ii) to make possible the use of the EFP method^{39–41} in molecular dynamics simulations involving a protein–solvent molecular system.

Acknowledgment. This work was supported by the Brazilian Research National Council (CNPq), the FAPERJ Agency, CNPq/IM-INOVAR, and MCT/PRONEX (Brazilian Government): Contract Grant Nos. 402003/3003-9, E26/171.401/01, 420.015/2005-1, and E-26/170.648/2004.

Supporting Information Available: The damping parameter values obtained for the 20 amino acids (files SM_Alphas_AMN_A.txt and SM_Alphas_med_AMN_B.txt) and the amino acids conformations used in this work (file SM_Alphas_AMN_A.txt). This material is available free of charge via the Internet at <http://pubs.acs.org>.

References and Notes

- (1) Russel, A. J.; Fersht, A. R. *Nature* **1987**, 328, 496.
- (2) Nakamura, H. *Q. Rev. Biophys.* **1996**, 29, 1.
- (3) Warshel, A.; Florián, J. *Proc. Natl. Acad. Sci. U.S.A.* **1998**, 95 (11), 5950.
- (4) Stone, A. J. *Chem. Phys. Lett.* **1981**, 83 (2), 233.
- (5) Stone, A. J.; Alderton, M. *Mol. Phys.* **1985**, 56 (5), 1047.
- (6) Chipot, C.; Angyan, J. G.; Maigret, B.; Scheraga, H. A. *J. Phys. Chem.* **1993**, 97, 9788.
- (7) Chipot, C.; Angyan, J. G.; Maigret, B.; Scheraga, H. A. *J. Phys. Chem.* **1993**, 97, 9797.
- (8) Gresh, N.; Claverie, P.; Pullman, A. *Int. J. Quantum Chem. Symp.* **1979**, 11, 253.
- (9) Gresh, N.; Guo, H.; Kafafi, S. A.; Salahub, D. R.; Roques, B. P. *J. Am. Chem. Soc.* **1999**, 121, 7885.
- (10) Day, P. N.; Jensen, J. H.; Gordon, M. S.; Webb, S. P.; Stevens, W. J.; Kraus, M.; Garmer, D.; Basch, H.; Cohen, D. *J. Chem. Phys.* **1996**, 105, 1968.
- (11) Jensen, H.; Gordon, M. S. *Mol. Phys.* **1996**, 89, 1313.
- (12) Jensen, H.; Gordon, M. S. *J. Chem. Phys.* **1998**, 108, 4772.
- (13) Gordon, M. S.; Freitag, M. A.; Bandyopadhyay, P.; Jensen, J. H.; Kairys, V.; Stevens, W. J. *J. Phys. Chem. A* **2001**, 105, 293.
- (14) Grigorenko, B. L.; Nemukhin, A. V.; Topol, I. A.; Burt, S. K. *J. Phys. Chem. A* **2002**, 106, 10663.
- (15) Matta, C. F.; Bader, R. F. W. *Proteins: Struct., Funct., Genet.* **2000**, 40, 310.
- (16) Molina, P. A.; Li, H.; Jensen, J. H. *J. Comput. Chem.* **2003**, 24, 1971.
- (17) Dardenne, L. E.; Werneck, A. S.; Oliveira Neto, M.; Bisch, P. M. *J. Comput. Chem.* **2001**, 22, 689.
- (18) Werneck, A. S.; Neto, M. O.; Maia, E. R. *J. Mol. Struct. (THEOCHEM)* **1998**, 427, 15.
- (19) Minikis, R. M.; Kairys, V.; Jensen, J. H. *J. Phys. Chem. A* **2001**, 105, 3829.
- (20) Dardenne, L. E.; Werneck, A. S.; Oliveira Neto, M.; Bisch, P. M. *Proteins: Struct., Funct., Genet.* **2003**, 52, 236.
- (21) Freitag, M. A.; Gordon, M. S.; Jensen, W. J. *J. Chem. Phys.* **2000**, 112 (17), 7300.
- (22) Piquemal, J. P.; Gresh, N.; Giessner-Prettre, C. *J. Phys. Chem. A* **2003**, 107, 10353.
- (23) Guo, H.; Gresh, N.; Roques, B. P.; Salahub, D. R. *J. Phys. Chem. B* **2000**, 104, 9746.
- (24) Tabacchi, G.; Mundy, C. J.; Hutter, J.; Parrinello, M. *J. Chem. Phys.* **2002**, 117 (4), 1416.
- (25) Kaminski, G. A.; Stern, H. A.; Berne, B. J.; Friesner, R. A.; Cao, Y. X.; Murphy, R. B.; Zhou, R.; Halgren, T. A. *J. Comput. Chem.* **2002**, 23, 1515.
- (26) Adamovic, I. A.; Freitag, M. A.; Gordon, M. S. *J. Chem. Phys.* **2003**, 118 (15), 6725.
- (27) Ledecq, M.; Lebon, F.; Durant, F.; Giessner-Prettre, C.; Marquez, A.; Gresh, N. *J. Phys. Chem. B* **2003**, 107, 10640.
- (28) Gresh, N.; Kafafi, S. A.; Truchon, J.; Salahub, D. R. *J. Comput. Chem.* **2004**, 25, 823.
- (29) Kaminski, G. A.; Stern, H. A.; Berne, B. J.; Friesner, R. A. *J. Phys. Chem. A* **2004**, 108, 621.
- (30) Chelli, R.; Schettino, V.; Procacci, P. *J. Chem. Phys.* **2005**, 122, 234107.
- (31) Donchev, A. G.; Subbotin, M. V.; Tarasov, O. V.; Tarasov, V. I. *Proc. Natl. Acad. Sci. U.S.A.* **2005**, 102 (22), 7829.
- (32) Gresh, N.; Piquemal, J.; Krauss, M. *J. Comput. Chem.* **2005**, 26, 1113.
- (33) Piquemal, J.; Cisneros, A.; Reinhardt, P.; Gresh, N.; Darden, T. A. *J. Chem. Phys.* **2006**, 124, 104101.
- (34) Morokuma, K. *J. J. Chem. Phys.* **1971**, 55, 1236.
- (35) Connolly, M. L. *Science* **1983**, 221 (4612), 709.
- (36) Press, W. H.; Teukolsky, S. A.; Vetterling, W. T.; Flannery, B. P. *Numerical Recipes*, 2nd ed.; Cambridge University Press: Cambridge, 1992; Chapter 10.
- (37) Schmidt, M. W.; Baldrige, K. K.; Boatz, J. A.; Elbert, S. T.; Gordon, M. S.; Jensen, J. H.; Koseki, S.; Matsunaga, N.; Nguyen, K. A.; Su, S.; Windus, T. L.; Dupuis, M.; Montgomery, J. A., Jr. *J. Comput. Chem.* **1993**, 14 (11), 1347.
- (38) De Magalhães, C. S.; Barbosa, H. J. C.; Dardenne, L. E. *Lect. Notes Comput. Sci.* **2004**, 3102, 368.
- (39) Li, H.; Netzloff, H. M.; Gordon, M. S. *J. Chem. Phys.* **2006**, 125, 194103.
- (40) Li, H.; Gordon, M. S. *Theor. Chem. Acc.* **2006**, 115, 385.
- (41) Li, H.; Gordon, M. S. *J. Chem. Phys.* **2007**, 126, 124112.